



**HAL**  
open science

## Numerical approach of grinding process in a stirred media mill

Romain Gers, Eric Climent, Dominique Legendre, Dominique Anne-Archard,  
Christine Frances

► **To cite this version:**

Romain Gers, Eric Climent, Dominique Legendre, Dominique Anne-Archard, Christine Frances. Numerical approach of grinding process in a stirred media mill. Symposium PARTEC2007, Mar 2007, Nuremberg, Germany. pp.0. hal-04105949

**HAL Id: hal-04105949**

**<https://hal.science/hal-04105949>**

Submitted on 25 May 2023

**HAL** is a multi-disciplinary open access archive for the deposit and dissemination of scientific research documents, whether they are published or not. The documents may come from teaching and research institutions in France or abroad, or from public or private research centers.

L'archive ouverte pluridisciplinaire **HAL**, est destinée au dépôt et à la diffusion de documents scientifiques de niveau recherche, publiés ou non, émanant des établissements d'enseignement et de recherche français ou étrangers, des laboratoires publics ou privés.

Symposium PARTEC2007, Nuremberg, Germany, 29/31.03.07

## Numerical approach of grinding process in a stirred media mill

 Romain Gers<sup>1,2</sup>, Eric Climent<sup>1</sup>, Dominique Legendre<sup>2</sup>, Dominique Anne-Archard<sup>2</sup>,  
Christine Frances<sup>1</sup>

1- Laboratoire de Génie Chimique UMR CNRS/INPT/UPS 5503, Toulouse France

2- Institut de Mécanique des Fluides de Toulouse UMR CNRS/INPT/UPS 5502

### ABSTRACT

Producing nanoparticles in dense suspensions can be achieved in a stirred media mill. However the mechanism of fragmentation in the mill is still not well understood and the process remains laborious because of the considerable energy needed. We focus on the numerical analysis of the global hydrodynamics in the mill for determining the parameters which control the efficiency of the collisions between grinding beads (impact velocities and orientation of the collision). The suspension flow is modelled with effective physical properties. We solve directly the Navier-Stokes equations in an axisymmetric two-dimensional domain. Then, we select some particular impact configurations of two spherical beads and simulate the flow motion during the film drainage.

### 1 INTRODUCTION

Stirred media mills have appeared to be an efficient way to produce nanoparticles. Particles are suspended in a fluid under high solid fraction conditions. In this device (fig. 1), the grinding volume is approximately filled up to 80 % with microbeads (200 $\mu$ m radius). The actual solid fraction is 50.4 % according to a random close packing of 63 % for the beads. The remaining volume contains a suspension of particles to be milled and the carrying fluid is usually an aqueous solution with surfactants. It is important to stabilize the suspension for preventing aggregation after grinding. A central rotating agitator (usually composed of several discs either perforated or not) induces a strong stirring within the suspension (typically, 2000-6000 rpm). Basically the particle fragmentation results from the capture of particles inside a zone of strong stress occurring when two grinding beads collide (frontal collisions in straining regions or oblique collisions induced by a local shear rate).

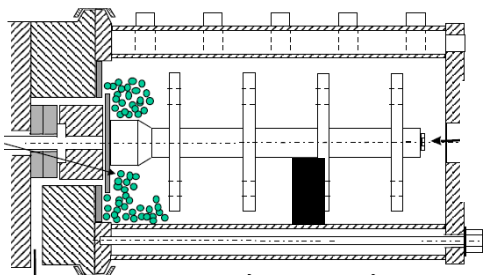


Figure 1: Sketch of a stirred media mill and definition of the simulation domain (black patch).

The mechanism of fragmentation is not well understood and the process remains laborious because of the large amount of mechanical energy needed. Also many experiments have revealed that the particle size achieves a steady distribution during the fragmentation process. It is important to achieve a basic knowledge of the grinding mechanisms for predicting the minimum achievable particle size. Indeed, limitations of the process may be mechanical, physico-chemical or related to the process itself. We want to focus on the hydrodynamic limitations of the particle size reduction. When two grinding beads collide, they induce a fluid motion in the gap (squeezing

outflow due to lubrication). Therefore most of the energy impact is dissipated in the fluid. The available energy is related to the fluid viscosity and the impact parameters. Also, only particles that remain in this active volume may be crushed. Experiments have shown that the particle size, the solid concentration of the suspension and the physico-chemical interactions between particle surfaces have a great importance during the size reduction process. However we don't know the role of each of these parameters regarding the impact velocity and the diameter of the grinding beads. We want to address the following questions: what is the mechanical limitation of the particle size reduction due to hydrodynamics and how it is parameterized by the physical properties of the suspension and the impact parameters of the grinding beads.

The purpose of our study is a precise analysis of the hydrodynamics in the mill in order to estimate the collision velocities between the grinding beads for each configuration (frontal or oblique collision). We want to quantify the available energy and the concentration of particles in the active volume of fragmentation. We investigate the hydrodynamics in the mill numerically, simulating the suspension flow by direct numerical solution of the Navier-Stokes equations for an equivalent fluid. This gives local information on the collision parameters of the grinding beads which are used in a second step to analyze the flow between two approaching beads.

### 2 NUMERICAL SIMULATIONS

The suspension (particles, beads and underlying fluid) is assumed to have a Newtonian behaviour. We assume that the flow is two-dimensional and that the effective fluid is incompressible.

$$\nabla \cdot \vec{v} = 0$$

$$\rho \left( \frac{\partial \vec{v}}{\partial t} + \vec{v} \cdot \nabla \vec{v} \right) = -\nabla P + \mu \Delta \vec{v}$$

where  $\rho$  is the effective fluid density,  $\vec{v}$  the fluid velocity,  $P$  the pressure,  $\mu$  the suspension viscosity. The equations correspond to the continuity equation and the momentum balance, respectively. We used a numerical code developed at the Institut de Mécanique des Fluides

de Toulouse [1] which solves the fluid motion equations on a staggered grid using finite volumes.

In these equations, the equivalent fluid properties are constant. We want to simulate the behaviour of the flowing phase, constituted by the suspension (fluid and particles to be crushed) and the grinding beads. Thus, we avoid the complexity of a multiphase flow simulation without losing the (global) specific characteristics of the fluid. The viscosity of the equivalent fluid is deduced from the Krieger-Dougherty model:

$$\mu = \mu_p \left( 1 - \frac{\phi}{\phi_m} \right)^{-\frac{5}{2} \phi_m}$$

where  $\mu_p$  is the viscosity of the particle suspension, which is considered as the carrying fluid for the grinding beads.  $\phi$  and  $\phi_m$  are respectively the volume fraction and the random close packing fraction (63%) for the grinding beads. The size ratio between the grinding beads and the particles of the suspension is larger than 10 and will increase during the size reduction process. Therefore we can assume that the bulk suspension can be considered as an equivalent fluid where the grinding beads are suspended. In a previous experimental study with  $\text{CaCO}_3$  particles ( $2700 \text{ kg/m}^3$ ), the viscosity  $\mu_p$  was determined to vary roughly from  $2.10^{-3} \text{ Pa.s}$  to  $0.1 \text{ Pa.s}$  for a  $\text{CaCO}_3$  mass fraction between 40 and 50%, depending on the dispersing agent concentration [3]. Combined with the density of each material, this leads to kinematical viscosity  $\mu/\rho$  around  $3.3 \cdot 10^{-4} \text{ m}^2/\text{s}$ .

Using geometric symmetries, we can simulate the flow in the domain showed on fig. 2 in axisymmetric reference framework. The simulation domain is bounded by the mill wall (on the right,  $r/\Delta R=5$ ), the shaft wall (on the left,  $r/\Delta R=0$ ) and two planes of symmetry (on the top,  $z/\Delta R=1.73$ , on the bottom,  $z/\Delta R=0$ ). The rotating disc is materialized by the dark rectangle. Physically, the dimensions of the mill are 26 mm for the width and 75 mm for the inner radius of the mill. The disc radius is 60 mm. The geometry is similar to the reactor simulated in Ref [2].

The disc is rotating with a constant tangential velocity which is normal to the visualization plane ( $r,z$ ) of Figs 2,3 and 4. Typically the rotation rate 955 rpm corresponds to a tangential velocity  $W_{\text{tip}}$  at the disc tip of 6 m/s. The global hydrodynamics is basically controlled by the Reynolds number and the geometry of the reactor. Therefore we chose the tangential velocity at the disc tip and the gap between the disc tip and the mill wall  $\Delta R$  as characteristic velocity and length scales respectively.

### 3 DISCUSSION

Practically, the cinematic viscosity is gradually decreased and each flow configuration obtained for a given viscosity is used as an initial condition for the lower viscosity. Each simulation corresponds to a distinct Reynolds number (see figures 2, 3 and 4). On these figures, the viscosities are  $1 \times 10^{-3}$ ,  $5 \times 10^{-4}$  and  $3.5 \times 10^{-4} \text{ m}^2/\text{s}$ , corresponding to Reynolds numbers equal to 90, 180 and 257, respectively. At low Reynolds number, the flow is purely tangential; we used a composite solution based on a solid body rotation and a pure Couette flow to initialize the transient evolution of the numerical solution.

Beyond a critical value of  $Re$ , secondary flows in the axial-radial plane ( $r,z$ ) appear because of the tangential velocity  $W_{\text{tip}}$  which generates a centrifugal instability near the disc. As the instability sets in, a toroidal vortex develops associated to the streamlines plotted in Fig. 2. For instance, when  $Re=257$  the velocity of the secondary flow ( $r,z$  plane) reaches a maximum velocity of 15%  $W_{\text{tip}}$ . This behaviour is strictly similar to the Couette-Taylor instability.

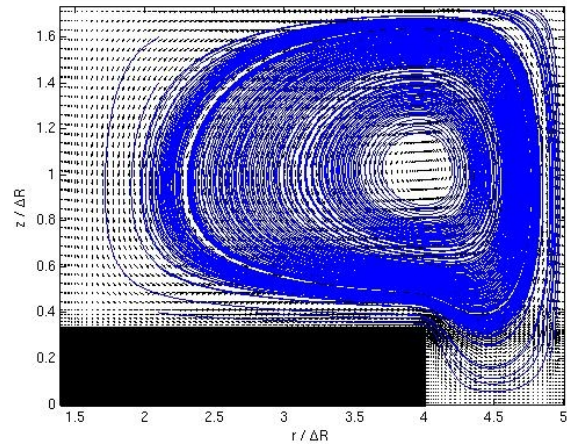


Figure 2: Secondary flows in the ( $r,z$ ) plane ( $Re = 90$ ).

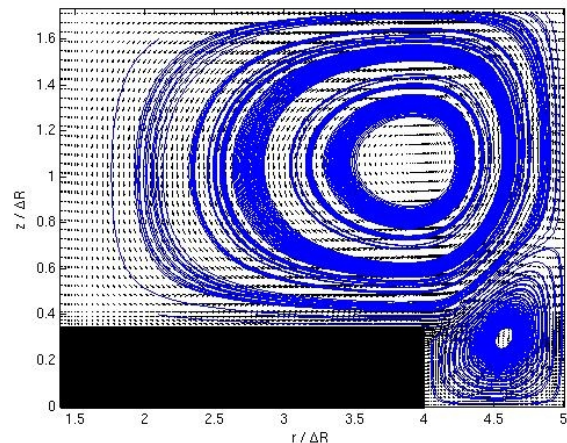


Figure 3: Secondary flows in the ( $r,z$ ) plane ( $Re = 180$ ).

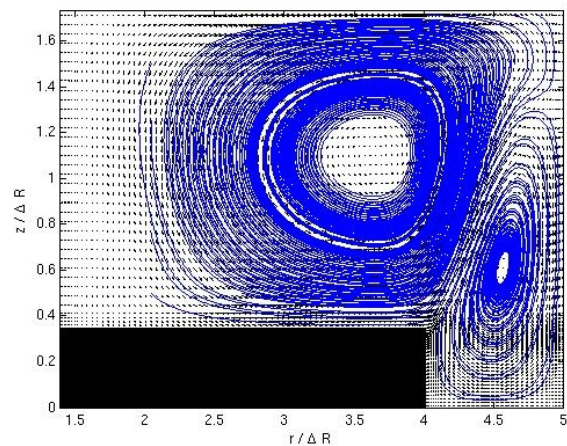


Figure 4: Secondary flows in the ( $r,z$ ) plane ( $Re = 257$ ).

It is interesting to note that the flow is drastically modified when the  $Re$  is further increased (Figs 2 and 3). We observe two contra-rotating vortices, one is located in

the gap between the rotating disc tip and the fixed outer cylinder and the largest one fills the remaining space of the reactor.

When Re increased from 180 to 257, the smallest vortex expands. It is known that this flow pattern may be unstable when the Reynolds number is further increased and bifurcates to a wavy oscillation in the tangential direction but we didn't investigate precisely this kind of flow transition yet.

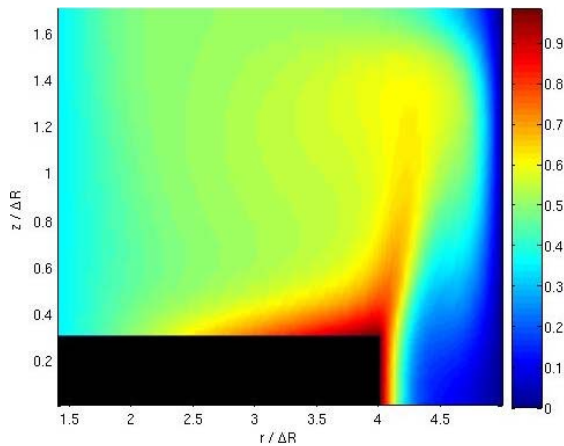


Figure 5: Level lines of the tangential velocity (Re=257)

In Figs. 5 and 6, we plotted level lines and profiles of the tangential velocity. Close to the rotating disk, the flow evolves like a solid body rotation ( $r/\Delta r < 4$ ) and then goes to zero on the fixed wall ( $r/\Delta r = 5$ ) which contributes to the centrifugal instability that controls the vortex strength of the secondary flow. The figure 6 shows more precisely the tangential velocity  $W(r)$  profile at the disc surface and at the symmetry axis between two discs when the Reynolds number Re is respectively equal to 180 and 257. We can see that these profiles logically differ when the Reynolds number is increased.

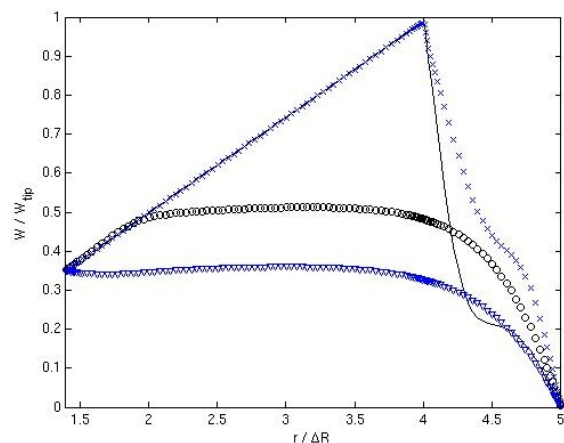


Figure 6: Radial profile of the tangential velocity at the surface of the disc (and blue crosses for Re = 180 for black line Re = 257) and at the symmetry axis between two discs (blue triangles for Re = 180 and dark circles for Re = 257)

Due to their low inertia, grinding beads and particles are expected to follow the streamlines of the flow. Collision of beads will be encountered in several configurations: frontal collision of the beads in straining regions of the flow, oblique collision due to local shear rate. The energy

involved in the process is not uniformly distributed in the mill and this may select some particular locations of efficient collisions leading to fragmentation of the particles.

High energy is located where the shear stress is large. The tangential velocity is the most important contribution to the kinetic energy in the mill. It is obvious that the maximum of energy can be found in planes perpendicular to the shaft and near the discs because the tangential velocity at the tip of the discs is the maximum velocity in the mill.

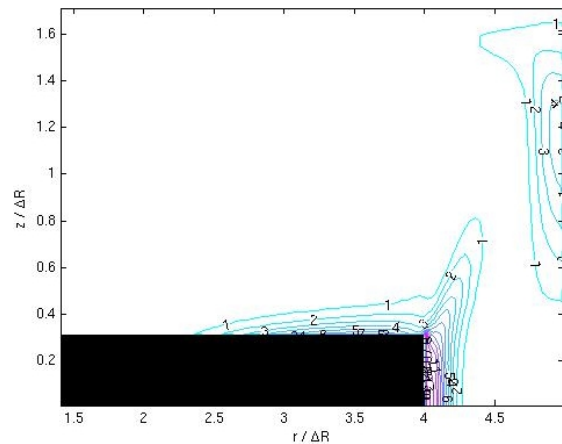


Figure 7: Level lines of the dimensionless specific power (Re = 257). The maximum value is around 13 close to the tip of the rotating disc.

The dimensionless specific power (local specific power scaled by the volume average specific power) is an alternative quantity to locate the energy dissipation in the mill [4]. This quantity is closely related to the local dissipation of fluid energy by viscous effects. In Figure 7, high levels of energy dissipation are confined in specific regions of the reactor, near the disc and near the mill wall. In these zones the most intense collisions are expected.

In order to quantify that the collisions induced by the shear stress in the disc plane ( $r, \theta$ ) are the more efficient (according to [5]), we used the streamlines to detect the local properties of collisions.

Based on a typical distance of 400  $\mu\text{m}$  (bead diameter) between two consecutive streamlines, we can extract the differential velocity between beads that would follow the fluid flow. It appears that the maximum intensity of the frontal collisions between a wall and a bead is weak when the inertia of the bead is neglected. This result is somehow related to the assumption of equivalent single phase flow. The relative velocity at impact for a frontal collision in the axial-radial plane ( $r, z$ ) reaches only 1.5% of  $W_{ip}$ . On the contrary, it reaches 10% of  $W_{ip}$  for an oblique impact in the radial-tangential plane ( $r, \theta$ ) and 4.6% in the ( $r, z$ ) plane. We see that the strength of collisions is larger for shear induced relative motion.

## 4 PERSPECTIVES

The main goal of the study on the global hydrodynamics in a stirred media mill was the estimation of relevant

parameters for the impact velocities between grinding beads in a binary collision. We found that the collisions induced by the strong shear in the disc plane ( $r, \theta$ ) are the most intense and therefore the most efficient for the fragmentation of suspended particles.

Based on this information, it is now possible to focus on the local simulation of collision events. The simulation approach is based on the direct solution of the Navier-Stokes equations between two spherical beads in motion. We use a boundary fitted mesh (Figure 8) evolving in time while the beads are approaching. The critical issue is the film drainage that may clear out the active volume of fragmentation from the suspended particles. We expect that the capture probability of suspended particles is related to operating conditions: particle size, local particle concentration and surface interactions.

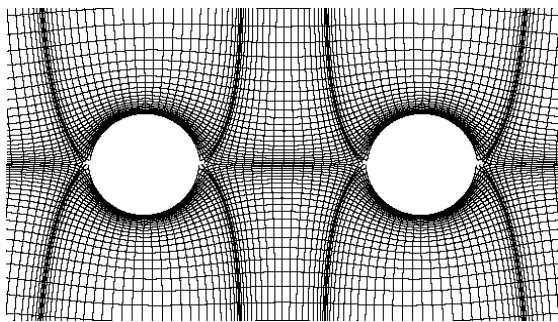


Figure 8: Boundary fitted mesh used in the simulation of a frontal collision.

As a first validation test, we simulate the flow around two spheres involved in a frontal collision at small Reynolds number ( $Re=0.01$ ). In that case, the Reynolds number is based on the bead radius, the approaching velocity and the suspension viscosity. The figure 9 shows the pressure field around the beads when the gap is equal to one diameter. We compared the force acting on the sphere obtained numerically with analytical solution of Stokes flow equations.

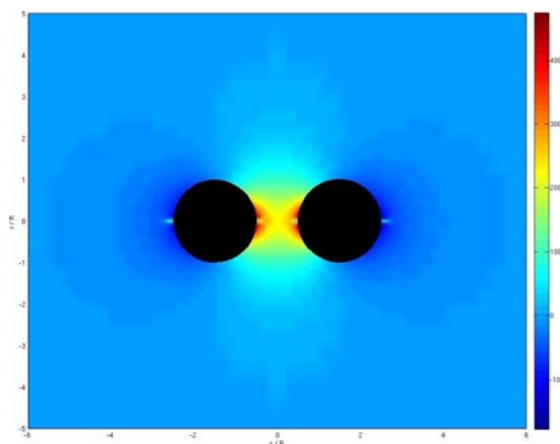


Figure 9: Pressure field around two approaching beads at low Reynolds number.

We found a good agreement. When the gap between both spheres gradually varies from 3 to 0.375 bead diameter, the force drastically increases due to viscous drag and a strong increase of the pressure in the fluid film. In the configuration of Stokes flows, fluid inertia is neglected and approaching beads can be simulated through

independent simulations on fixed grids. Time-dependence occurs only because of the unsteady motion of the boundary conditions.

The ongoing work will be devoted to the extension of the numerical method for the solution of the Navier-Stokes equations on a deforming mesh. Also we need to develop a new numerical procedure for the mesh generation for extremely close particles (less than 10% of the bead diameter). When the gap is short, mesh cells are highly stretched and numerical inaccuracy may occur.

## REFERENCES

- [1] Legendre, Magnaudet & Mougin, Hydrodynamic interactions between two spherical bubbles rising side by side in a viscous liquid, 2003, *J. Fluid Mech.* Vol. 497 p.133-166
- [2] Theuerkauf & Schwedes, Investigation of motion in stirred media mills, 2000, *Chem. Eng. Science* 23
- [3] Frances, Anne-Archard, Propriétés physiques de suspensions denses de particules submicroniques obtenues par nanobroyage en voie humide. 4<sup>ème</sup> Colloque Sciences et Technologie des Poudres, 4-6 Mai 2004, Compiègne, France. Récents progrès en Génie des Procédés n°91, ISBN 2-910239-65-9
- [4] Blecher & Schwedes, Energy distribution and particle trajectories in a grinding chamber of a stirred ball mill, 1996, *Int. J. Miner. Process.* 44-45 p.617-627
- [5] Kwade, Determination of the most important grinding mechanisms in stirred media mills by calculating stress intensity and stress number, 1999, *Powder Tech.* 105 p.382-388

## Acknowledgements

We are very grateful for the support of the National Research Agency under the program ACI-Nanobroyage and the local support of the cooperative structure of joint research FERMaT.